

Inter-cluster Voltage Balancing Control of Modular Multilevel Cascaded Converter Under Unbalanced Grid Voltage

Oghenewogaga Oghorada, *Member, IEEE*, Li Zhang, *Member, IEEE*, Ayodele Esan, Dickson Egbune, and Julius Uwagboe

Abstract—This paper presents a novel inter-cluster direct current (DC) capacitor voltage balancing control scheme for the single-star configured modular multilevel cascaded converter (MMCC)-based static synchronous compensator (STATCOM) under unbalanced grid voltage. The negative-sequence component of grid voltage at the point of common connection (PCC) causes unbalanced active power flow in the phase limbs of converter. This leads to the imbalance of DC voltages of the sub-module capacitors across the MMCC phases, and consequently, the malfunction of converter. The proposed solution is to inject both negative-sequence current (NSC) and zero-sequence voltage (ZSV) into the phase limbs of MMCC. A quantification factor Q_f is used to achieve the sharing of inter-cluster active power between the NSC and ZSV injection methods. Accurate determination of the quantification factor has been presented. In addition to maintaining the DC voltages of sub-module capacitor across the MMCC phases balanced, it also prevents the overcurrent and overvoltage of converter by injecting NSC and ZSV with the right proportion. The control scheme is validated on a 3.54 kV 1.2 MVA power system using MMCC-based STATCOM with 3-level bridge cells as sub-modules. The results show that the proposed scheme provides superior effectiveness in eliminating the voltage imbalance of DC capacitor in the phase limb while maintaining low voltage and current ratings.

Index Terms—Low-voltage ride through (LVRT), single-star bridge converter (SSBC), static synchronous compensator (STATCOM), modular multilevel cascaded converter (MMCC), quantification factor.

I. INTRODUCTION

UNBALANCED voltage in a power system can be caused by symmetrical faults, and uneven distribution of loads such as electric traction drives, start-up operation of large industrial drives, asymmetric transmission impedances,

and blown fuses in three-phase capacitor banks [1]. The integration of renewable energy generators into the distribution network via power electronic converters poses challenges to the grid voltage quality [2]. As a concern, it is required that all power converters connected on the grid lines should not only operate properly under normal grid voltage conditions, but also ride-through the abnormal situations and support the grid voltage during transient grid faults.

The modular multilevel cascaded converter (MMCC) is a type of voltage source converter (VSC) that is an alternative to conventional two-level VSCs in medium- and high-voltage applications such as battery energy storage system (BESS) and static compensators (STATCOMs) [3]-[8]. With its modular structure, the MMCC offers benefits such as scalability, good waveform quality at a low switching frequency, and fault-tolerance. Its modular nature can also reach any required voltage level without step-up transformers [8], [9].

The MMCC-based STATCOM can compensate reactive power under balanced conditions [4], [10]. Under balance grid condition, the average cluster power of converter is balanced and equal, which does not cause any inter-cluster imbalance. However, with the occurrence of voltage fault, it faces peculiar challenges. In the three-phase three-wire case, the negative-sequence component in the unbalanced voltage at the point of common connection (PCC) inevitably induces unbalanced active power in the converter [11]. This results from the product of positive-sequence current and negative-sequence voltage. This unbalanced power of the converter phase makes the voltages of sub-module capacitor across the MMCC clusters unequal, i. e., inter-cluster voltage imbalance. Note that there is also the usual voltage imbalance between sub-module capacitors within a phase limb, i. e., intra-cluster voltage imbalance [12], which can be solved by DC-bus feedback control using DC components. If not properly controlled, this inter-cluster voltage imbalance will cause the STATCOM to inject distorted currents into the power system. Besides, excessive voltage drifts of the DC capacitor may overstress the converter switches to a damaging extent [13].

References [13]-[21] have proposed the injection of ZSV to achieve inter-cluster balancing control for the star-connected MMCC by adding a sinusoidal zero-sequence voltage (ZSV) in the neutral point of the star-connected converter to cancel out the unbalance active power. Another method for inter-cluster balancing control method for single-star bridge

Manuscript received: October 29, 2019; revised: March 20, 2020; accepted: September 11, 2020. Date of CrossCheck: July 23, 2020. Date of online publication: October 22, 2020.

This article is distributed under the terms of the Creative Commons Attribution 4.0 International License (<http://creativecommons.org/licenses/by/4.0/>).

O. Oghorada (corresponding author), A. Esan, D. Egbune, and J. Uwagboe are with the Department of Electrical & Information Engineering, Landmark University, Omu-Aran, Kwara State, Nigeria (e-mail: oghorada.oghenewogaga@lmu.edu.ng; esan.ayodele@lmu.edu.ng; egbune.dickson@lmu.edu.ng; Uwagboe.julius@lmu.edu.ng).

L. Zhang is with University of Leeds, Leeds, United Kingdom (e-mail: l.zhang@leeds.ac.uk).

DOI: 10.35833/MPCE.2019.000129



converter (SSBC)-MMCC is the injection of negative-sequence current (NSC) [11]. Each of these injection techniques has its limitations. Injecting ZSV can push the phase voltages of the converter to operate above the linear modulation mode [15]. For the NSC method, it may result in high maximum current, which could damage power semiconductor devices.

The steady-state operation of SSBC under unbalanced conditions is discussed in [14], [22], [23]. It does not meet the requirement of low-voltage ride through (LVRT), which is a short response time normally below 20-80 ms [24], [25]. Only SSBC-STATCOM has been investigated under LVRT condition [11], [26], [27], and no paper has analyzed the influence of ZSV and NSC injection techniques on the voltage and current rating requirements to the level of voltage imbalance.

This paper proposes a novel control scheme for phase-cluster voltage balance of the single star-connected MMCC-STATCOMs under unbalanced voltage conditions. Different from the conventional methods which inject only NSC and ZSV, the proposed scheme injects both NSC and ZSV to overcome the problem of overcurrent and over-modulation peculiar to NSC and ZSV, respectively. In this scheme, a quantification factor Q_f is determined which aids the sharing of the inter-cluster active powers between NSC and ZSC methods in a way that prevents overcurrent and over-modulation. A detailed power flow analysis of the star-connected MMCC under unbalanced voltage condition is analyzed. The influence of the unbalance voltage level on the voltage and current ratings of this converter topology are investigated. The MMCC sub-module considered in this paper is the three-level H-bridge (3L-HB). A digital simulation test result is presented to validate the proposed scheme in this paper.

II. CIRCUIT STRUCTURE OF STAR-CONNECTED MMCC-STATCOM

Figure 1 shows the system connection of the star-connected MMCC-STATCOM. Each cluster consists of N 3L-HBs or five-level flying capacitor (5L-FC) full-bridge sub-modules connected in series as shown in Fig. 1. For the SSBC, the three filter reactors are connected between the MMCC terminals and the PCC of the power system. The DC capacitor voltages $V_{DC,mm}$ ($m = a, b, c$; $n = 1, 2, \dots, N$) in a phase cluster of the converter need to be maintained balanced under unbalanced voltage conditions. For this configured MMCC, the output phase voltages and currents of the converter are expressed in (1) and (2), respectively.

$$v_{mM} = v_{sm}^+ + v_{sm}^- + v_0 = V_+ \sin\left(\omega t + \varphi_{V_+} - k \frac{2\pi}{3}\right) + V_- \sin\left(-\omega t + \varphi_{V_-} - k \frac{2\pi}{3}\right) + V_0 \sin(\omega t + \varphi_{V_0}) \quad (1)$$

$$i_m = i_m^+ + i_m^- = I_+ \sin\left(\omega t + \varphi_{I_+} - k \frac{2\pi}{3}\right) + I_- \sin\left(-\omega t + \varphi_{I_-} - k \frac{2\pi}{3}\right) \quad (2)$$

where v_{mM} is the converter cluster voltage; $k=0, 1, 2$ for $m = a, b, c$; +, -, and 0 represent the positive, negative, and zero-sequence components, respectively; V_+ , V_- , I_+ , and I_- are the

positive and negative-sequence voltage and current magnitudes, respectively; V_0 is the ZSV magnitude; and φ_{V_+} , φ_{V_-} , φ_{V_0} , φ_{I_+} , φ_{I_-} are the phase angles of the ZSVs, positive and negative currents, respectively.

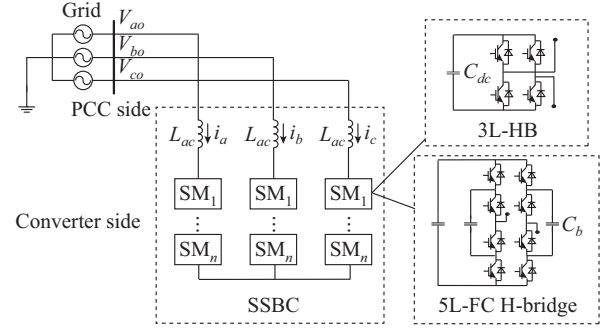


Fig. 1. System configuration of star-connected MMCC-STATCOM.

III. POWER FLOW ANALYSIS OF STAR-CONNECTED MMCC-STATCOM

To achieve the voltage balancing control of single-star MMCC sub-module capacitor, the power flow affecting the inter-phase DC capacitor voltage balancing is analyzed. The instantaneous and average power across each phase of MMCC-STATCOM is achieved by multiplying (1) and (2). The phase cluster powers are expressed as:

$$\begin{cases} P_m = 0.5(P_{Cm}^{++} + P_{Cm}^{--} + P_{Cm}^{+-} + P_{Cm}^{-+} + P_{Cm}^{0+} + P_{Cm}^{0-}) \\ P_{Cm}^{++} = V_+ I_+ \cos(\varphi_{V_+} - \varphi_{I_+}) \\ P_{Cm}^{--} = V_- I_- \cos(\varphi_{V_-} - \varphi_{I_-}) \\ P_{Cm}^{+-} = q \frac{1}{2} V_+ I_- \cos(\varphi_{V_+} + \varphi_{I_-}) + r \frac{\sqrt{3}}{2} V_+ I_- \sin(\varphi_{V_+} + \varphi_{I_-}) \\ P_{Cm}^{-+} = q \frac{1}{2} V_- I_+ \cos(\varphi_{V_-} + \varphi_{I_+}) + r \frac{\sqrt{3}}{2} V_- I_+ \sin(\varphi_{V_-} + \varphi_{I_+}) \\ P_{Cm}^{0+} = -q \frac{1}{2} V_0 I_+ \cos(\varphi_{V_0} - \varphi_{I_+}) - r \frac{\sqrt{3}}{2} V_0 I_+ \sin(\varphi_{V_0} - \varphi_{I_+}) \\ P_{Cm}^{0-} = q \frac{1}{2} V_0 I_- \cos(\varphi_{V_0} + \varphi_{I_-}) - r \frac{\sqrt{3}}{2} V_0 I_- \sin(\varphi_{V_0} + \varphi_{I_-}) \end{cases} \quad (3)$$

where $q = -2, 1, 1$, and $r = 0, 1, -1$ for phases $m = a, b, c$, respectively.

Across this converter, P_{Cm}^{++} and P_{Cm}^{--} contribute to the overall active powers of the converter while the rest sums up to zero as shown in (4), where the subscript "T" represents the total power across the three clusters.

$$\begin{cases} P_T^{++} = P_{Ca}^{++} + P_{Cb}^{++} + P_{Cc}^{++} = 1.5 V_+ I_+ \cos(\varphi_{V_+} - \varphi_{I_+}) \\ P_T^{--} = P_{Ca}^{--} + P_{Cb}^{--} + P_{Cc}^{--} = 1.5 V_- I_- \cos(\varphi_{V_-} - \varphi_{I_-}) \\ P_T^{+-} = P_{Ca}^{+-} + P_{Cb}^{+-} + P_{Cc}^{+-} = 0 \\ P_T^{-+} = P_{Ca}^{-+} + P_{Cb}^{-+} + P_{Cc}^{-+} = 0 \\ P_T^{0+} = P_{Ca}^{0+} + P_{Cb}^{0+} + P_{Cc}^{0+} = 0 \\ P_T^{0-} = P_{Ca}^{0-} + P_{Cb}^{0-} + P_{Cc}^{0-} = 0 \end{cases} \quad (4)$$

From (4), the ZSV does not contribute to the overall control of DC capacitor voltage. Thus, for a balanced system, the overall active powers in (4) are equally contributed by their respective phases.

The phase average active powers are defined in (5). The average active phase power in (5) only flows within the MMCC-STATCOM, but not between the power system and

the STATCOM. In addition to the overall active power, the overall average reactive power based on instantaneous power

$$\left\{ \begin{array}{l} \begin{array}{l} \left[\begin{array}{l} P_{Ca}^{+-} \\ P_{Cb}^{+-} \\ P_{Cc}^{+-} \end{array} \right] = 0.5 \begin{bmatrix} -V_+ \cos \varphi_{V_+} & V_+ \sin \varphi_{V_+} \\ 0.5(V_+ \cos \varphi_{V_+} + \sqrt{3} V_+ \sin \varphi_{V_+}) & 0.5(-V_+ \sin \varphi_{V_+} + \sqrt{3} V_+ \cos \varphi_{V_+}) \\ 0.5(V_+ \cos \varphi_{V_+} - \sqrt{3} V_+ \sin \varphi_{V_+}) & 0.5(-V_+ \sin \varphi_{V_+} - \sqrt{3} V_+ \cos \varphi_{V_+}) \end{bmatrix} \begin{bmatrix} I_- \cos \varphi_{I_-} \\ I_- \sin \varphi_{I_-} \end{bmatrix} \\ \left[\begin{array}{l} P_{Ca}^{-+} \\ P_{Cb}^{-+} \\ P_{Cc}^{-+} \end{array} \right] = 0.5 \begin{bmatrix} -V_- \cos \varphi_{V_-} & V_- \sin \varphi_{V_-} \\ 0.5(V_- \cos \varphi_{V_-} + \sqrt{3} V_- \sin \varphi_{V_-}) & 0.5(-V_- \sin \varphi_{V_-} + \sqrt{3} V_- \cos \varphi_{V_-}) \\ 0.5(V_- \cos \varphi_{V_-} - \sqrt{3} V_- \sin \varphi_{V_-}) & 0.5(-V_- \sin \varphi_{V_-} - \sqrt{3} V_- \cos \varphi_{V_-}) \end{bmatrix} \begin{bmatrix} I_+ \cos \varphi_{I_+} \\ I_+ \sin \varphi_{I_+} \end{bmatrix} \\ \left[\begin{array}{l} P_{C0a} \\ P_{C0b} \\ P_{C0c} \end{array} \right] = 0.5 \begin{bmatrix} I_+ \cos \varphi_{I_+} & I_+ \cos \varphi_{I_+} \\ 0.5(-I_+ \cos \varphi_{I_+} + \sqrt{3} I_+ \sin \varphi_{I_+}) & 0.5(-I_+ \sin \varphi_{I_+} - \sqrt{3} I_+ \cos \varphi_{I_+}) \\ 0.5(-I_+ \cos \varphi_{I_+} - \sqrt{3} I_+ \sin \varphi_{I_+}) & 0.5(-I_+ \sin \varphi_{I_+} + \sqrt{3} I_+ \cos \varphi_{I_+}) \end{bmatrix} + \\ \left[\begin{array}{l} I_- \cos \varphi_{I_-} & -I_- \cos \varphi_{I_-} \\ 0.5(-I_- \cos \varphi_{I_-} - \sqrt{3} I_- \sin \varphi_{I_-}) & 0.5(I_- \sin \varphi_{I_-} - \sqrt{3} I_- \cos \varphi_{I_-}) \\ 0.5(-I_- \cos \varphi_{I_-} + \sqrt{3} I_- \sin \varphi_{I_-}) & 0.5(I_- \sin \varphi_{I_-} + \sqrt{3} I_- \cos \varphi_{I_-}) \end{bmatrix} \end{array} \right\} \begin{bmatrix} V_0 \cos \varphi_{V_0} \\ V_0 \sin \varphi_{V_0} \end{bmatrix} \quad (5)$$

$$\left\{ \begin{array}{l} Q_T^{++} = Q_a^{++} + Q_b^{++} + Q_c^{++} = -1.5 V_+ I_+ \sin(\varphi_{V_+} - \varphi_{I_+}) \\ Q_T^{-} = Q_a^{-} + Q_b^{-} + Q_c^{-} = -1.5 V_- I_- \sin(\varphi_{V_-} - \varphi_{I_-}) \end{array} \right. \quad (6)$$

From (5), there are three-degree possibilities of control freedoms for this converter including the positive-sequence currents ($I_+ \cos \varphi_{I_+}, I_+ \sin \varphi_{I_+}$), NSC ($I_- \cos \varphi_{I_-}, I_- \sin \varphi_{I_-}$), and ZSV (v_0). In achieving overall active and reactive power flow, the positive-sequence currents ($I_+ \cos \varphi_{I_+}, I_+ \sin \varphi_{I_+}$) are

theory [28] is expressed in (6).

applied. Thus, there are only two possible degrees of control freedoms, i.e., the NSC and ZSV, which are available for inter-cluster voltage balancing control.

IV. CONTROL SCHEME

Figure 2 shows the control block diagram of the MMCC-STATCOM, where v_{dcm} is the cluster DC capacitor voltage; and v_{mMref} is the converter cluster voltage reference.

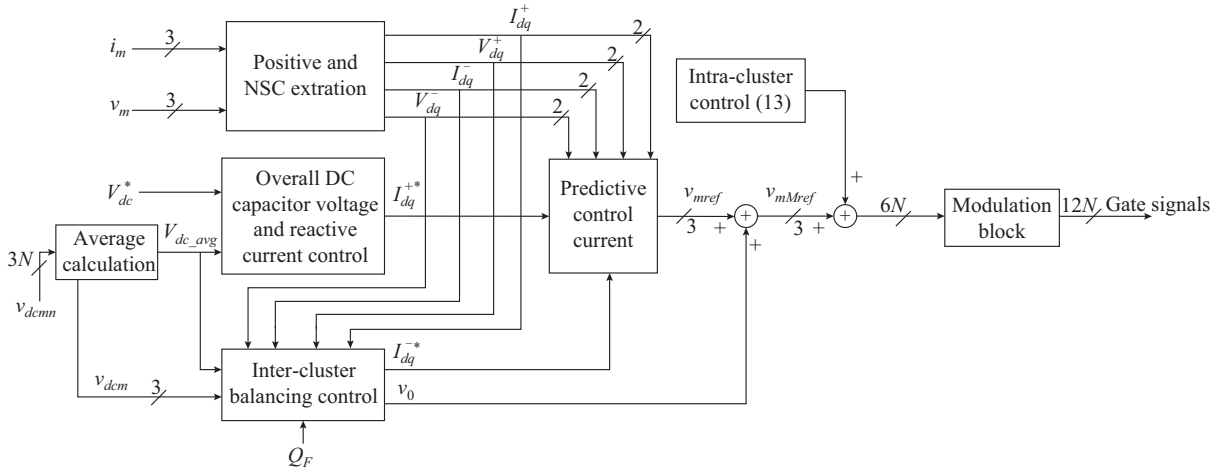


Fig. 2. Control block diagram of MMCC-STATCOM under unbalanced voltage condition.

This control scheme is divided into three sections: overall control, inter-cluster DC capacitor voltage control, and intra-cluster DC capacitor voltage control. The overall control regulates the overall DC capacitor voltage and reactive power injection. As analyzed above, the overall average active and reactive power are influenced by converter currents. Thus, the overall DC capacitor voltages and average reactive power are controlled by the positive-sequence currents. The positive-sequence current, NSC, and ZSV are the degrees of control freedom that influence the control of the inter-cluster

power flow. $V_{dq}^+, V_{dq}^-, I_{dq}^+, I_{dq}^-$ are the measured positive- and negative-sequence voltage and current, respectively; I_{dq}^{+*} and I_{dq}^{-*} are the controlled positive-sequence current and NSC signal, respectively; V_{dc_avg} is the average value of all three-phase sub-module DC voltages; v_{dcm} is the sub-module DC capacitor voltage; Q_F is the quantification factor; and v_{mref} is the converter voltage reference signal. The afore-mentioned inter-cluster average active phase power flow is discussed below.

A. Overall DC Capacitor Voltage and Reactive Power Control

This controller is used to provide the active power required to compensate for power losses of the power semiconductor switches of star-connected MMCC, and to regulate the overall DC capacitor voltages to their required values. Also, it controls the reactive power to be injected into the power system by the converter. This regulation is achieved using the PI regulator as shown in Fig. 3.

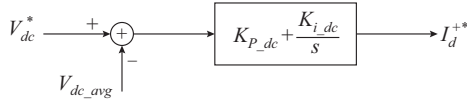


Fig. 3. Overall DC capacitor voltage.

The output of this controller generates the direct component of the positive-sequence current. In order to control the injection of reactive power, the reactive current is calculated.

$$\begin{cases} i_d^{+*} = \left(K_{P_dc} + \frac{K_{I_dc}}{s} \right) (V_{dc}^* - V_{dc_avg}) \\ I_q^{+*} = \frac{2Q_{ref}}{3V_d^+} \end{cases} \quad (7)$$

where K_{P_dc} and K_{I_dc} are the proportional and integral gains of the proportional-integral (PI) regulator, respectively; V_{dc}^* is the desired reference value of the DC-link; and Q_{ref} is the reactive power reference. In order to avoid excessive phase current in the MMCC-STATCOM under the condition of LVRT, a fixed quadrature current is applied.

B. Inter-cluster Voltage Balancing Control

The inter-phase DC capacitor voltages of each phase may differ because of the unequal average active power resulting from unbalanced grid voltage condition. The average active cluster power is given as:

$$P_{Cm} = P_{Cm}^{+-} + P_{Cm}^{-+} + P_{Cm}^0 \quad (8)$$

Equation (8) shows that the average cluster active power comprises the positive and NSC power components and ZSV power components. Since the positive-sequence current have been applied for the overall controller, the NSC and ZSV are used for regulating the inter-cluster average active power. When harnessing both methods in regulating the clus-

ter average active power, Q_F is used to effectively allocate the various share of the NSC active power P_{Cm}^{+-} and ZSV active power P_{Cm}^0 by firstly transforming the three phases into α - β frame as follows:

$$\begin{cases} \begin{bmatrix} P_{Ca}^{+-*} \\ P_{Cb}^{+-*} \\ P_{Cc}^{+-*} \end{bmatrix} = \begin{bmatrix} 1 & -\frac{1}{2} & -\frac{1}{2} \\ 0 & -\frac{\sqrt{3}}{2} & \frac{\sqrt{3}}{2} \end{bmatrix} \begin{bmatrix} P_{Ca}^{+-*} \\ P_{Cb}^{+-*} \\ P_{Cc}^{+-*} \end{bmatrix} \\ \begin{bmatrix} P_{Ca}^{0*} \\ P_{Cb}^{0*} \\ P_{Cc}^{0*} \end{bmatrix} = \begin{bmatrix} 1 & -\frac{1}{2} & -\frac{1}{2} \\ 0 & -\frac{\sqrt{3}}{2} & \frac{\sqrt{3}}{2} \end{bmatrix} \begin{bmatrix} P_{Ca}^{0*} \\ P_{Cb}^{0*} \\ P_{Cc}^{0*} \end{bmatrix} \end{cases} \quad (9)$$

Both P_{Cm}^{+-} and P_{Cm}^0 are expressed in (11) using Q_F as:

$$\begin{cases} P_{Cm}^{+-*} = Q_F (P_{Cm}^* - P_{Cm}^{-+}) \\ P_{Cm}^{0*} = (1 - Q_F) (P_{Cm}^* - P_{Cm}^{-+}) \end{cases} \quad (10)$$

where $m = \alpha, \beta$. The ZSV and NSC are expressed as:

$$\begin{cases} \begin{bmatrix} V_0 \cos \varphi_{V0} \\ V_0 \sin \varphi_{V0} \end{bmatrix} = \frac{2}{I_+^2 - I_-^2} \cdot \begin{bmatrix} I_+ \cos \varphi_{I_+} + I_- \cos \varphi_{I_-} & -I_+ \sin \varphi_{I_+} - I_- \sin \varphi_{I_-} \\ I_+ \sin \varphi_{I_+} - I_- \sin \varphi_{I_-} & I_+ \cos \varphi_{I_+} - I_- \cos \varphi_{I_-} \end{bmatrix} \begin{bmatrix} P_{Ca}^{0*} \\ P_{Cb}^{0*} \end{bmatrix} \\ V_0 = \sqrt{(V_0 \cos \varphi_{V0})^2 + (V_0 \sin \varphi_{V0})^2} \\ \varphi_{V0} = \tan^{-1} \left(\frac{V_0 \sin \varphi_{V0}}{V_0 \cos \varphi_{V0}} \right) \\ \begin{bmatrix} I_- \cos \varphi_{I_-} \\ I_+ \cos \varphi_{I_+} \end{bmatrix} = \frac{2}{V_+} \begin{bmatrix} -\cos \varphi_{V_+} & -\sin \varphi_{V_+} \\ \sin \varphi_{V_+} & -\cos \varphi_{V_+} \end{bmatrix} \begin{bmatrix} P_{Ca}^{+-*} \\ P_{Cb}^{+-*} \end{bmatrix} \end{cases} \quad (11)$$

Figure 4 illustrates the control scheme of the proposed inter-cluster voltage balancing control. The positive-sequence current average active power P_{Cm}^{+-} is subtracted from the cluster average active powers P_{Cm}^* generated from PI controllers. The resulting values are used in determining the NSCs and ZSV depending on the choice of Q_F .

The NSCs generated from the NSC inter-cluster controller along with the positive-sequence currents from the overall DC capacitor voltage and reactive current controller are fed to the predictive current controller to generate v_{mref} .

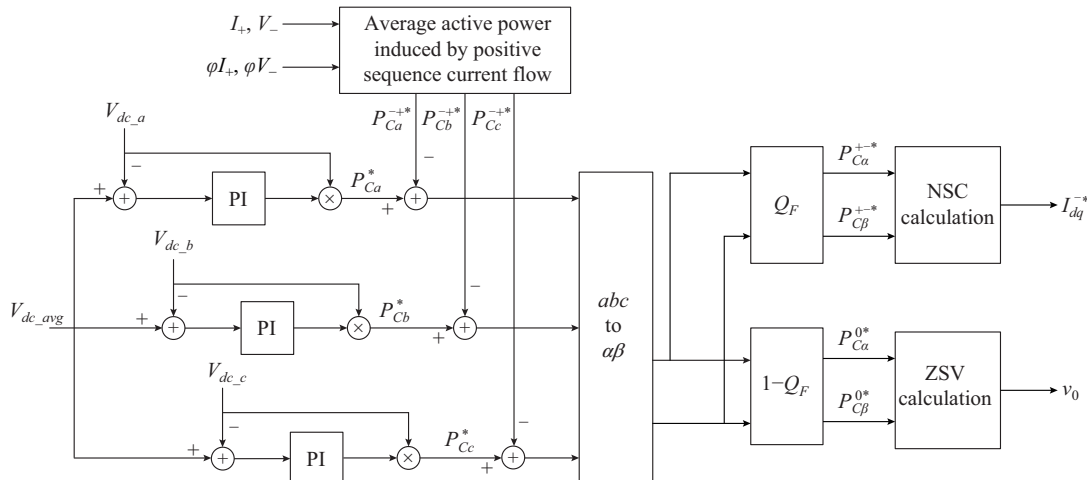


Fig. 4. Inter-cluster balancing control using quantification factor for sharing.

The ZSV calculated from the inter-cluster balancing controller is added to v_{mref} as shown in Fig. 2.

The intra-cluster DC voltage controller is implemented to regulate the active power across each sub-module across a particular phase to actualize DC capacitor voltage balancing of each sub-module at that phase cluster. The intra-cluster control for each sub-module at a particular phase v_{Smn}^{in} is:

$$v_{Smn}^{in} = \left(k_p^{cin} + \frac{k_i^{cin}}{s} \right) (V_{dcm} - V_{dcmn}) \quad (12)$$

where k_p^{cin} and k_i^{cin} are the proportional and integral gain constants, respectively. The output of the intra-cluster control is added to v_{mMref} and the new converter voltage reference signals are applied to phase-shifted PWM (PS-PWM) [29] to generate the converter gate signals.

C. Determination of Quantification Factor

The value of Q_F is determined by ensuring that the converter modulation index and converter rated current are not exceeded. Among the two inter-cluster balancing methods, the ZSV method is chosen to be superior over the NSC technique in the determination of Q_F .

This is because the NSC technique achieves inter-cluster voltage balancing control by injecting this current into the power system, which is not preferred because of the power quality deterioration.

The ZSV technique is chosen to solely achieve inter-cluster voltage balancing control if the maximum of the three-phase converter output voltages is less or equal to the maximum available voltage:

$$V_{\max} \leq m_{ref} V_{dc_ref} \quad Q_F = 0 \quad (13)$$

$$V_{\max} = \max(v_{aM}, v_{bM}, v_{cM}) \quad (14)$$

where v_{aM} , v_{bM} , and v_{cM} are the converter cluster voltages; V_{dc_ref} is the converter reference DC voltage; and m_{ref} is the modulation ratio reference with a maximum value of 1, since PS-PWM is applied in this paper.

Under severe fault conditions, the maximum available voltage may be less than the maximum magnitude of the converter output voltages, i.e., $V_{\max} \geq m_{ref} V_{dc_ref}$. To avoid over-modulation, a new value of Q_F is determined as:

$$Q_F = 1 - \frac{m_{ref} V_{dc_ref}}{V_{\max}} \quad (15)$$

Figure 5 shows a flowchart for the determination of Q_F .

V. STAR-CONNECTED MMCC RATINGS UNDER UNBALANCED VOLTAGE CONDITIONS

The operation range and ratings of the star-connected MMCC are analyzed under voltage unbalanced condition. This analysis is based on the integration of both ZSV and NSC techniques using the quantification factor Q_F in sharing the inter-cluster phase active power. The degree of voltage unbalance $K_{vr} = V_-/V_+$ is used in these investigations. To determine the DC capacitor rated voltage V_{dc_rated} and maximum current I_{\max} of the delta MMCC, the influence of methods are considered. Equations (16)-(19) are applied [15]:

$$V_{dc_rated} = \max |V_{mM}| \leq N V_{dc} \quad (16)$$

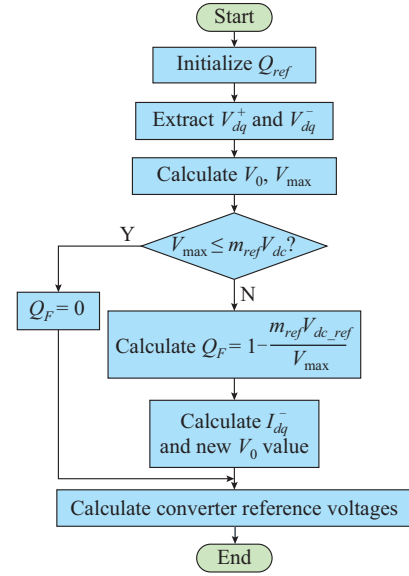


Fig. 5. Flowchart for determination of Q_F .

$$V_{mM} = v_m + v_0 + L \underbrace{\frac{di_m}{dt}}_{V_f} + Ri_m = V_{mM} \sin(\omega t + \phi_m) \quad (17)$$

$$i_m = i_+ + i_- \quad (18)$$

$$I_{\max} = \max |I_m| \quad (19)$$

where V_{dc} is the cluster individual module DC-link voltage; N is the number of modules per phase; V_f is the voltage drop across the MMCC filter; $m = a, b, c$; i_m is the phase cluster current; i_+ is the compensated positive-sequence current; and i_- is the NSC.

In this analysis, $Q_F = 0, 0.5$, and 1 are applied across the converter, respectively. For $Q_F = 0$, only ZSV injection method is applied. For $Q_F = 1$, only NSC injection technique is used. For $Q_F = 0.5$, 50% of their total inter-cluster power is shared between both techniques.

Figure 6(a)-(c) highlights the voltage and current rating requirements for the star-connected STATCOM with $Q_F = 0, 0.5$, and 1 , $0 \leq K_{vr} \leq 0.9$. Figure 6(a) shows that for $Q_F = 0$, the voltage and current rating at $K_{vr} = 0.8$ are 1.8 p.u. and 1 p.u., respectively, where the ZSV injection technique is solely applied. For $Q_F = 0.5$ in Fig. 6(b), both the voltage and current ratings at $K_{vr} = 0.8$ are 1.4 p.u. and 1.4 p.u.. Figure 6(c) shows that the voltage and current rating requirements using only the NSC injection method, i.e., $Q_F = 1$, are 1 p.u. and 1.8 p.u., respectively. From this analysis, it is seen that combining the ZSV method with the NSC method provides better voltage rating requirement than solely using the ZSV method. Likewise, this proposed scheme also provides a better current rating requirement than solely using the NSC method. Thus, by employing the proposed scheme, the voltage and current rating requirements of the star-connected MMCC-based STATCOM are increased by 0.4 p.u., which has a direct implication on the voltage and current ratings of switching devices and DC capacitors.

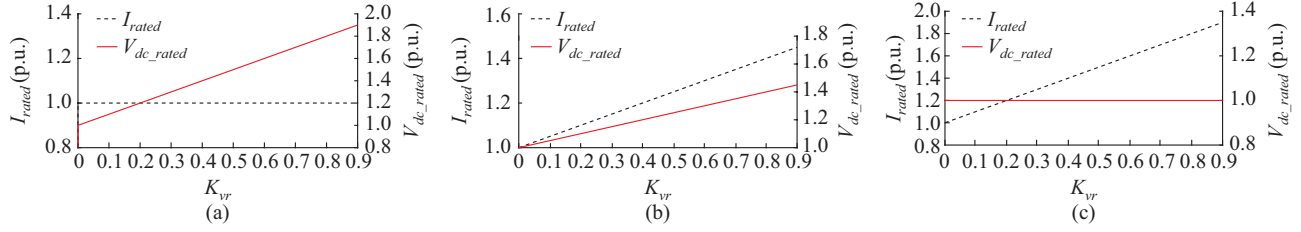


Fig. 6. DC-link cluster voltage and cluster current ratings of SSBC-STATCOM with respect to K_{vr} with $\phi_{V_r}=0$. (a) $Q_F=0$. (b) $Q_F=0.5$. (c) $Q_F=1$.

VI. RESULTS AND DISCUSSION

The system arrangements are shown in Fig. 1, where three cascaded 3L-HB star-connected MMCC is tested with the overall control scheme shown in Fig. 2 in a MATLAB/Simulink environment. Tables I and II show the power system and controller parameters, respectively. The controller parameters are chosen based on the cut-off frequency of 10 Hz and phase margin of 60° . The step response of the PI controller is shown in Fig. 7, where the percentage overshoot is 5% with a rise time of 4 ms and settling time of 20 ms, respectively.

TABLE I
MMCC POWER SYSTEM PARAMETERS

Symbol	Quantity	Value
V_s	Grid root-mean-square voltage	3536 V
S	Grid rated power	1.2 MVA
C_{sm}	Sub-module capacitance	1.12 mF
L_{ac}	Reactance of filter	8 mH
R_{ac}	Resistance of filter	2 Ω
V_{dc}	Sub-module DC voltage	2000 V
N	Number of sub-modules per phase	3
f_c	Carrier frequency	1000 Hz
f_s	Sampling frequency	10000 Hz

TABLE II
MMCC CONTROLLER PARAMETERS

Symbol	Quantity	Value
$K_{p_{dc}}, K_{i_{dc}}$	Overall DC voltage control	2, 20
$K_{p_{c}}, K_{i_{c}}$	Inter-cluster control	1, 10
$K_{p_{cin}}, K_{i_{cin}}$	Intra-cluster control	0.5, 5

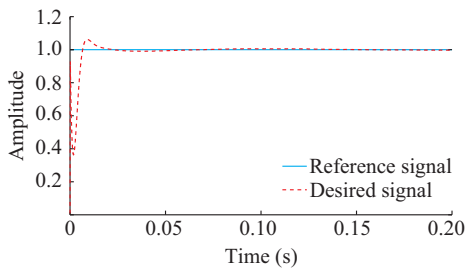


Fig. 7. Step response of PI controller.

The overall DC bus voltage control generates the positive-sequence active current reference signal I_d^{+*} and the reactive power reference generates the positive-sequence reactive current I_q^{+*} . Under the LVRT condition, the STATCOM injects

constant quadrature current ($I_q^{+*} = 80$ A) to aid the power system. The inter-cluster balancing control technique is tested under 100% voltage sag in phase a as illustrated in Fig. 8.

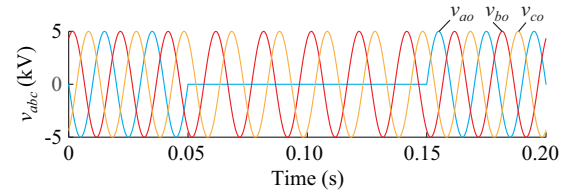


Fig. 8. Voltage waveform of power system under 100% voltage sag in phase a during 100 ms.

The converter current is rated as $I_{rated} = 90$ A and the maximum modulation ratio m_{ref} is set to be 1.0. $V_{dc,ref}$ is fixed at 2000 V. To validate the effectiveness of the proposed scheme in determining Q_F value between 0 and 1, the ZSV method ($Q_F=0$) and negative-sequence method ($Q_F=1$) are subjected to this condition.

Figure 9 shows the test results using the ZSV technique for inter-cluster voltage balancing control. The phase cluster power is compensated by only zero-sequence average active power, which determines the ZSV as shown in Fig. 9(a). Figure 9(b) shows the converter reference modulation ratios. The over-modulation of the converter reference voltages leads to not maintaining the references values of the sub-module DC capacitor voltages, as illustrated in Fig. 9(c). As shown in Fig. 9(d), the STATCOM phase currents injected to the power system are balanced.

The test results in implementing inter-cluster balancing control using only the NSC are shown in Fig. 10. The phase cluster power is compensated using only the negative-sequence average active power, which determines the NSC as shown in Fig 10(a). Figure 10(b) shows that the maximum current is 105 A ($1.16I_{rated}$). When no overcurrent protection technique is activated, there will be thermal breakdown of semiconductor switches. Figure 10(c) shows that the modulation ratios of the converter reference voltages are below $m_{ref}=1$, which results in the sub-module capacitor voltages kept at their reference values. Figure 10(d) shows the sub-module capacitor voltages which are maintained within $\pm 10\%$ of the rated values.

Figure 11 shows the test results using the proposed technique for the inter-cluster voltage balancing control. To overcome the problem posed by ZSV and NSC methods, the proposed scheme determines that $Q_F=0.25$, i.e., the inter-cluster unbalanced active power is shared between both ZSV and NSC with proportions of 75% and 25%, respectively.

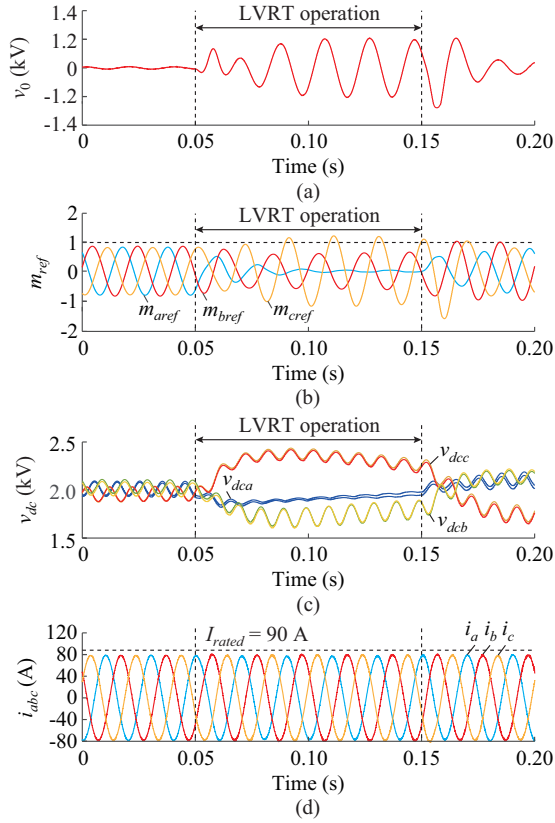


Fig. 9. Simulation result using ZSV injection technique. (a) ZSV. (b) Converter modulation references. (c) Inter-cluster DC sub-module capacitor voltages. (d) Converter phase currents.

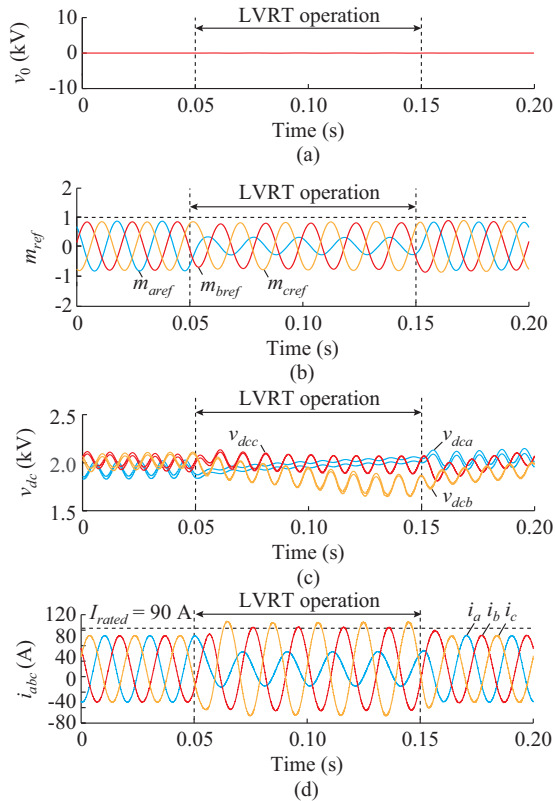


Fig. 10. Simulation result using NSC injection technique. (a) ZSV. (b) Converter modulation references. (c) Inter-cluster DC sub-module capacitor voltages. (d) Converter phase currents.

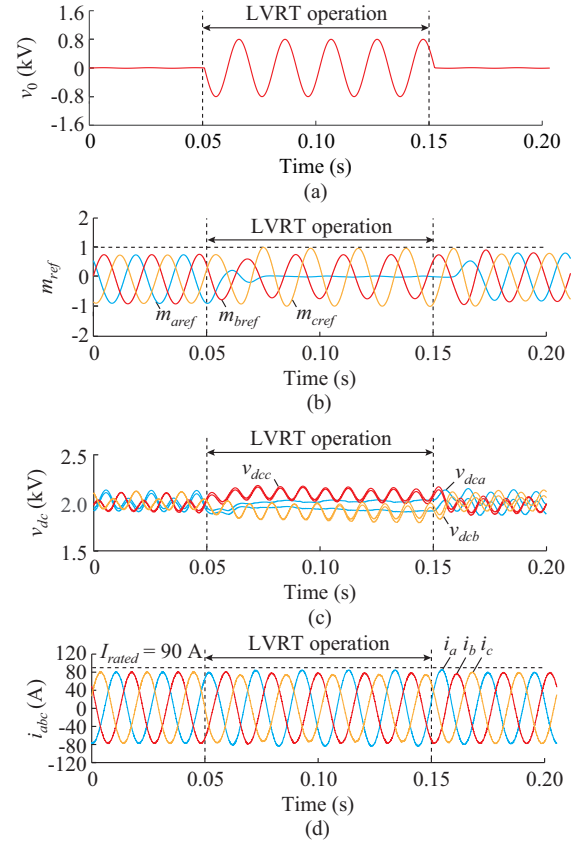


Fig. 11. Simulation result using proposed technique. (a) ZSV. (b) Converter modulation references. (c) Inter-cluster DC sub-module capacitor voltages. (d) Converter phase currents.

By comparing Fig. 11(a) and Fig. 9(a), the magnitude of the ZSV for the proposed scheme is lower than solely using the ZSV injection technique. The maximum current injected into the power system is observed to be within the rated current as illustrated in Fig. 11(b). The maximum modulation ratio of the converter voltage reference is also within the modulation ratio reference as shown in Fig. 11(c). The sub-module DC capacitor voltages are maintained at the DC capacitor voltage reference as shown in Fig. 11(d), because the converter reference voltage modulation ratios are not over-modulated.

The over-modulation of the converter reference voltage and converter over-current may occur when inter-cluster active power balancing control technique of either ZSV or NSC is applied under LVRT condition.

The proposed inter-cluster voltage balancing control method has the effectiveness of both techniques using a quantification factor Q_F to provide reliable reactive power support to the power system under LVRT condition.

VII. CONCLUSION

The inter-cluster voltage balancing control of the star-connected STATCOM is of critical concern, especially under unbalanced voltage conditions. This paper presents an inter-cluster voltage balancing control technique that manages the limitation of both ZSV and NSC injection techniques of over-modulation and overcurrent, respectively. The relation-

ship between the active power flow and inter-cluster DC capacitor voltages are discussed. These power flow analysis and the details of the proposed scheme are presented. The effectiveness of this proposed scheme is achieved by determining the quantification factor Q_F which integrates both conventional methods ZSV and NSC. The influence of the quantification factor Q_F and the degree of voltage unbalance K_v on the voltage and current ratings of the star-connected MMCC-STATCOM has been discussed. The simulation results have shown that the proposed scheme maintains the sub-module DC capacitor voltages at their reference values, and maintains the maximum current and converter reference voltage modulation ratios within their rated values.

REFERENCES

- [1] O. J. K. Oghorada, C. J. Nwobu, and L. Zhang, "Control of a single-star flying capacitor converter modular multi-level cascaded converter (SSFCC-MMCC) STATCOM for unbalanced load compensation," in *Proceedings of 8th IET International Conference on Power Electronics, Machines and Drives (PEMD 2016)*, Glasgow, UK, Apr. 2016, pp. 1-6.
- [2] O. J. K. Oghorada and L. Zhang, "Control of a modular multi-level converter STATCOM for low voltage ride-through condition," in *Proceedings of IECON 2016 42nd Annual Conference of the IEEE Industrial Electronics Society*, Florence, Italy, Oct. 2016, pp. 3691-3696.
- [3] H. Akagi, "Classification, terminology, and application of the modular multilevel cascade converter (MMCC)," *IEEE Transactions on Power Electronics*, vol. 26, no. 11, pp. 3119-3130, Nov. 2011.
- [4] K. Sano and M. Takasaki, "A transformer less DSTATCOM based on a multi-voltage cascade converter requiring no DC sources," *IEEE Transactions on Power Electronics*, vol. 27, no. 6, pp. 2783-2795, Nov. 2011.
- [5] M., Hagiwara, R. Maeda, and H. Akagi, "Application of a modular multilevel cascade converter (MMCC-SDBC) to a STATCOM," *Electrical Engineering in Japan*, vol. 131, no. 12, pp. 1433-1441, Nov. 2011.
- [6] C. Nwobu, I. B. Efika, O. J. K. Oghorada *et al.*, "A modular multilevel flying capacitor converter-based STATCOM for reactive power control in distribution systems," in *Proceedings of 2015 17th European Conference on Power Electronics and Applications (EPE'15 ECCE-Europe)*, Geneva, Switzerland, Sept. 2015, pp. 1-9.
- [7] B. Gultekin and E. Muammer, "Cascaded multilevel converter based transmission STATCOM: system design methodology and development of a 12 kV \pm 12 Mvar power stage," *IEEE Transactions on Power Electronics*, vol. 28, no. 11, pp. 4930-4950, Jan. 2013.
- [8] H. Akagi, S. Inoue, and T. Yoshii, "Control and performance of a transformer less cascade PWM STATCOM with star configuration," *IEEE Transactions on Industry Applications*, vol. 43, no. 4, pp. 1041-1049, Jul. 2007.
- [9] J. Zhang, S. Xu, Z. Din *et al.*, "Hybrid multilevel converters: topologies, evolutions and verifications," *Energies*, vol. 12, no. 4, pp. 1-29, Jan. 2019.
- [10] H. Huang, O. J. K. Oghorada, L. Zhang *et al.*, "Active harmonic current elimination and reactive power compensation using modular multilevel cascaded converter," in *Proceedings of 2017 19th European Conference on Power Electronics and Applications (EPE'17 ECCE Europe)*, Warsaw, Poland, Sept. 2017, pp. 1-11.
- [11] S. Chou, B. Wang, S. Chen *et al.*, "Average power balancing control of a STATCOM based on the cascaded H-bridge PWM converter with star configuration," *IEEE Transactions on Industry Applications*, vol. 50, no. 6, pp. 3893-3901, Nov. 2014.
- [12] P. Sochor and H. Akagi, "Theoretical comparison in energy-balancing capability between star- and delta-configured modular multilevel cascade inverters for utility-scale photovoltaic systems," *IEEE Transactions on Power Electronics*, vol. 31, no. 3, pp. 1980-1992, Jul. 2015.
- [13] O. J. K. Oghorada and L. Zhang, "Analysis of star and delta connected modular multilevel cascaded converter-based STATCOM for load unbalanced compensation," *International Journal of Electrical Power & Energy Systems*, vol. 95, pp. 341-352, Feb. 2018.
- [14] T. J. Summers, R. E. Betz, and G. Mirzaeva, "Phase leg voltage balancing of a cascaded H-bridge converter based STATCOM using zero sequence injection," in *Proceedings of 2009 13th European Conference on Power Electronics and Applications (EPE'09 ECCE-Europe)*, Barcelona, Spain, Sept. 2009, pp. 1-10.
- [15] O. J. K. Oghorada and L. Zhang, "Unbalanced and reactive load compensation using MMCC-based STATCOMs with third-harmonic injection," *IEEE Transactions on Industrial Electronics*, vol. 66, no. 4, pp. 2891-2902, Jun. 2018.
- [16] H. Huang, O. J. K. Oghorada, L. Zhang *et al.*, "Harmonics and unbalanced load compensation by a modular multilevel cascaded converter active power conditioner," *The Journal of Engineering*, vol. 17, pp. 3778-3783, Jan. 2019.
- [17] Y. Yu, G. Konstantinou, B. Hredzak *et al.*, "Power balance optimization of cascaded H-bridge multilevel converters for large-scale photovoltaic integration," *IEEE Transactions on Power Electronics*, vol. 31, no. 2, pp. 1108-1120, Feb. 2015.
- [18] H. Chen, P. Wu, C. Lee *et al.*, "ZSV injection for DC capacitor voltage balancing control of the star-connected cascaded H-bridge PWM converter under unbalanced grid," *IEEE Transactions on Industry Applications*, vol. 51, no. 6, pp. 4584-4594, Nov. 2015.
- [19] S. N. Duarte, F. T. Ghatti, P. M. de Almeida *et al.*, "Zero sequence voltage compensation of a distribution network through a four-wire modular multilevel static synchronous compensator," *International Journal of Electrical Power & Energy Systems*, vol. 109, pp. 57-72, Jul. 2019.
- [20] M. Xiao, F. Wang, Z. He *et al.*, "Power control and fault ride-through capability analysis of cascaded star-connected SVG under asymmetrical voltage conditions," *Energies*, vol. 12, no. 12, pp. 1-18, Jan. 2019.
- [21] E. Behrouzian and M. Bongiorno, "Investigation of negative-sequence injection capability of cascaded H-bridge converters in star and delta configuration," *IEEE Transactions on Power Electronics*, vol. 32, no. 2, pp. 1675-1683, Apr. 2016.
- [22] R. E. Betz and T. J. Summers, "Using a cascaded H-bridge STATCOM for rebalancing unbalanced voltages," in *Proceedings of 2007 7th International Conference on Power Electronics, Daegu, South Korea*, Oct. 2007, pp. 1219-1224.
- [23] R. E. Betz, T. Summers, and T. Furney, "Symmetry compensation using a H-bridge multilevel STATCOM with zero sequence injection," in *Proceedings of the 2006 IEEE Industry Applications Conference 41st IAS Annual Meeting*, Tampa, USA, Oct. 2006, pp. 1724-1731.
- [24] E.ON Netz GmbH, *Requirements for Off Grid Connections in the E.ON Netz Network*. Bayreuth: E.ON Press, Apr. 2008.
- [25] M. Altin, O. Goksu, R. Teodorescu *et al.*, "Overview of recent grid codes for wind power integration," in *Proceedings of 2010 12th International Conference on Optimization of Electrical and Electronic Equipment*, Basov, Romania, May 2010, pp. 1152-1160.
- [26] H. Chen and P. Cheng, "A DC bus voltage balancing technique for the cascaded H-bridge STATCOM with improved reliability under grid faults," *IEEE Transactions on Industry Applications*, vol. 53, no. 2, pp. 1263-1270, Mar. 2017.
- [27] C. Lee, H. Chen, C. Wang *et al.*, "A peak current limit control technique in low-voltage ride through operation of the star-connected cascaded H-bridges converter," in *Proceedings of 2014 IEEE Energy Conversion Congress and Exposition (ECCE)*, Pittsburgh, USA, Sept. 2014, pp. 505-512.
- [28] H. Akagi, E. H. Watanabe, and M. Aredes, *Instantaneous Power Theory and Applications to Power Conditioning*. Hoboken: John Wiley & Sons, 2017.
- [29] O. J. K. Oghorada, L. Zhang, B. A. Esan *et al.*, "Carrier-based sinusoidal pulse-width modulation techniques for flying capacitor modular multi-level cascaded converter," *Heliyon*, vol. 5, no. 12, pp. 1-16, Dec. 2019.

Oghenewogaga Oghorada received the B.Eng. degree in electrical engineering from Igbinedion University, Okada, Nigeria, in 2009. He received the M.Sc. and Ph.D. degrees in electronic/electrical engineering from University of Leeds, Leeds, UK, in 2012 and 2017, respectively. He is currently a Lecturer with the Department of Electrical and Information Engineering, Landmark University, Omu-Aran, Nigeria. His research interests include modulation and control of power converters, multilevel converters, modular multilevel converters, flexible alternating current transmission system (FACTS) devices, high-voltage direct current (HVDC) transmission systems, renewable energy systems, and energy management.

Li Zhang received the Ph.D. degree from Bradford University, Bradford, UK, in 1985. She has been a Research Associate in Oxford University, Oxford, UK, and a Lecturer and now Associate Professor in the School of Electronics and Electrical Engineering in the University of Leeds, Leeds, UK.

She became a Visiting Professor with Chongqing University, Chongqing, China, in 2006. She is an Associate Editor for IEEE Transactions on Power Electronics and has also been an Associate Editor for IET Proceedings on Power Electronics in 2014-2017. Her current research interests include power electronic converters and applications for power systems, FACTS devices, and renewable sourced generators.

Ayodele Esan received the Bachelor's degree in electrical and electronics engineering from Landmark University, Omu-Aran, Nigeria, in 2015, and the master's degree in electrical and electronics engineering from Covenant University, Canaanland Ota, Nigeria, in 2019. He currently works as a Lecturer in the Department of Electrical and Information Engineering at Landmark University. His research interests include distributed energy generation, energy economics, microgrid designs, energy analytics, and forecasting using machine learning techniques.

Egbune Dickson received the B.Eng. degree in electrical/electronic engi-

neering in Edo State University, Ekpoma, Nigeria, in 1998. He received the M.Sc. degree in computer science and M.Eng. degree in electronic and telecommunication both in University of Benin, Benin, Nigeria, in 2006 and 2008, respectively. He is currently pursuing the Ph.D. degree in Landmark University, Omu-Aran, Nigeria. He is also lecturing in the Department of Electrical and Information Engineering in Landmark University. His current research interests include spatial modulation techniques for wireless communication.

Julius Uwagboe received his Post Graduate Diploma (PGD) in electrical electronic engineering from the Federal University of Technology Akure, Akure, Nigeria, Higher National Diploma (HND) and National Diploma (ND) in electrical and electronics engineering technology from Auchi Polytechnic, Auchi, Nigeria. He is a Registered Member of the Nigerian Association of Technologist in Engineering (NATE). His research interests include renewable energy sources, energy economics, and power electronics.